A Reduced Order Model for Preliminary Design and Performance Prediction of Tapered Inducers: Comparison with Numerical Simulations

Luca d'Agostino[1], Lucio Torre[2], Angelo Pasini[3], Damiano Baccarella[4], A. Cervone[5] and Andrea Milani[6]

ALTA S.p.A. - Via Gherardesca, 5 - 56121 Ospedaletto, Pisa, Italy

The article recalls the recent development of a reduced order model for the preliminary design, geometric definition and noncavitating performance prediction of tapered-hub, variable-pitch, mixed-flow inducers, and illustrates its application to a typical three-bladed, high-head inducer for liquid propellant rocket engines. The mean axisymmetric flow field at the trailing edge of the inducer blades and the noncavitating head coefficient at both design and off-design conditions are then compared with those obtained from the numerical flow simulations generated by a commercial CFD code. Together with earlier experimental validations, the results dramatically confirm the capability of the proposed model to generate interpretative and useful engineering solutions of the inducer preliminary design problem at a negligible fraction of the computational cost required by 3D numerical simulations.

Nomenclature

b	blade thickness
c	blade chord
c_a	full-blade axial length
D	diffusion factor
L	axial length
N	number of blades
r	radial coordinate
r_H	inducer hub radius
r_T	inducer tip radius
s	azimuthal blade spacing
$\boldsymbol{u}$	flow velocity
u	radial flow velocity
v	azimuthal flow velocity
w	axial flow velocity
z	axial coordinate

[1] Professor, Aerospace Engineering Department, Pisa University, AIAA Member; luca.dagostino@ing.unipi.it
[2] Project Manager, ALTA S.p.A., AIAA Member; l.torre@alta-space.com
[3] Ph.D. Student, Aerospace Engineering Department, Pisa University - Project Engineer, ALTA S.p.A., AIAA Member; a.pasini@alta-space.com
[4] Project Engineer, ALTA S.p.A., AIAA Member; d.baccarella@alta-space.com
[5] Project Manager, ALTA S.p.A., AIAA Member; a.cervone@alta-space.com
[6] Project Engineer, ALTA S.p.A., AIAA Member; a.milani@alta-space.com

β_b blade angle evaluated w.r.t. the normal to the axial direction

β discharge flow angle

γ blade angle from axial direction

$\delta°$ discharge flow deviation angle

σ blade solidity $= c/s$

Φ flow coefficient

Ψ , Ψ_t static and total head coefficients

Ω inducer rotational speed

Superscripts

$\tilde{\boldsymbol{u}}$ slip flow velocity

Subscripts

D design conditions

T tip radius

H hub radius

le blade leading edge

te blade trailing edge

$\delta°$ flow deviation angle

1 upstream station (1)

2 downstream station (2)

Acronyms

BVP boundary value problem

CFD computational fluid dynamics

2D two-dimensional

3D three-dimensional

I. Introduction

AXIAL inducers are often used upstream of the centrifugal stage in rocket propellant feed turbopumps in order to avoid unacceptable cavitation, improve the suction performance and reduce the propellant tank pressure and weight. The main purpose of inducers consists in sufficiently pressurizing the flow for the main pump to operate satisfactorily. Compared to centrifugal pump impellers, typical inducers have fewer blades (usually 3 or 4), lower flow coefficients (from 0.05 to 0.1), larger stagger angles (70 to 85 deg from the axial direction) and significantly higher blade solidities (between 1.5 and 2.5). Long blades with small angles of attack provide ample time and room for the collapse of the cavitation bubbles and for the gradual exchange of energy with the flow. The resulting configuration, even though beneficial from the standpoint of cavitation performance, results in relatively low values of the inducer efficiency due to the highly viscous, turbulent and dissipative flow inside the blade passages.

In spite of the great importance of this kind of turbomachines for the rocket engine designers, not many 3D theoretical models have been proposed for providing efficient predictions of the pumping performance of axial inducers, probably due to the difficulty of adequately describing the complex flow field inside the blades. Designers often refer to simple "rules of thumb", or to the general indications of design manuals, such as the one published by NASA (Jakobsen[1]). In the last decades, numerical simulation of the complex 3D features of inducer flows has emerged has a promising tool for design validation and refinement (see, as an example, Ashihara et al.[2]; Kang et al.[3]), but its use in the early stages of design and for the geometric definition of the inducers still remains impractical.

Conversely, a number of 2D reduced order models for the prediction of the noncavitating flow in turbopump inducers are illustrated by Brennen[4,5]. These models are based on linear and radial cascade analyses with semi-empirical inclusion of flow deviation and viscous effects. Three-dimensional corrections for inlet flow prerotation, tip leakage and discharge flow are also indicated. A second class of models has been aimed at the prediction of the effects of cavitation on inducer performance (Stripling & Acosta[6]; Brennen & Acosta[7]; Brennen[8]). These models are essentially two-dimensional, where cavitation is assimilated to a vapor layer on the blade or a mixture of bubbles and liquid. Early studies opened the way to a number of more recent analyses capable of better understanding and predicting the major flow instabilities affecting cavitating inducers (Tsujimoto et al.[9,10]; Watanabe et al.[11]; d'Agostino & Venturini-Autieri[12,13]; Semenov et al.[14]).

Some earlier analyses of single and two phase flow in inducers have been carried out, among others, by Cooper[15]. More recently, Lakshminarayana[16] addressed the problem of performance prediction of noncavitating inducers by the combined use of a simplified radial equilibrium analysis and the Euler equation. Viscous effects are taken into account through an empirical loss coefficient deduced from the reported performance of inducers documented in the literature. Indications on the effects of solidity and number of blades are also provided.

At Alta S.p.A., Pisa, Italy, Bramanti et al.[17] developed a simplified model based on the traditional throughflow theory approximations with empirical corrections for incidence, friction and deviation losses of the flow through the inducer blades. The model proved to be in good agreement with the reported performance of several inducers tested in different facilities worldwide and represented the basis for the development of the analytical model illustrated in this paper and in a previous one (d'Agostino et al.[18]).

One of the main objectives in designing an axial inducer for rocket applications is the definition of a geometry capable of generating a progressively increasing head rise in the axial direction, thus limiting cavitating phenomena to the initial part of the inducer. The reduced order model proposed by d'Agostino et al.[18] offers the possibility of jointly determining the inducer hub and blade geometries as functions of a limited number of geometric input data (see Figure 1).

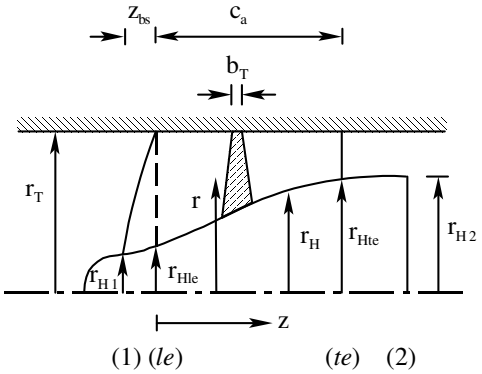

Figure 1. Inducer schematic and nomenclature.

Suitable redefinition of the diffusion factor for bladings with non-negligible radial flow allows for controlling the blade loading and evaluating the flow blockage effects of the boundary layers developing on the blade surfaces. The incompressible, inviscid, irrotational flow in the blade channels is approximated as the superposition of a fully-guided axisymmetric flow with radially uniform axial velocity and a 2D cross-sectional slip velocity correction (see Figure 2).

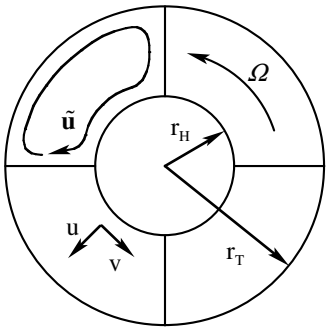

Figure 2. Schematic of the 2D cross-sectional slip velocity correction in the inducer blade channels.

Boundary layer blockage affects the velocity field, contributing to modify the axial schedules of hub-taper and blade pitch necessary to satisfy the irrotationality assumption. In order to obtain a more accurate prediction of the noncavitating performance, the velocity field for application of the incompressible isentropic Euler equation has been corrected for the nonidealities introduced by inlet flow incidence losses, turbulent duct losses and flow deviation at the inducer trailing edge.

In d'Agostino et al.[18], the model has been validated by comparing its results with the experimental data obtained from two space inducers tested in Alta's Cavitating Pump Rotordynamic Test Facility (CPRTF), as well as from a number of inducers documented in the open literature. In the present paper, the potential of the model as a design tool will be shown by illustrating its application to the preliminary geometric definition and performance analysis of a mixed-flow three-bladed inducer. For this inducer, the noncavitating performance and the flow field evaluated by the model will be compared to the results obtained by a CFD numerical simulation at design and moderately off-design conditions.

II. Discussion of Model Results

A. Inducer Geometry Generation

The reduced order model described in d'Agostino et al.[18] has been implemented in a fast and versatile MATLAB® numerical code, in order to be appropriately used for the design of new tapered-hub, variable-pitch inducers. Although the present version of the model has been developed for inducers with cylindrical tip housing and tapered hub, it can be easily adapted to the case of tapered blade tip and hub radii.

The starting point of the design process is represented by the required values for the main inducer geometrical and operational parameters: number of blades, tip radius, inlet tip blade angle, inlet and outlet hub radii, axial length and design flow coefficient. A first approximation of the tapered hub and blade geometry is carried out by simply neglecting boundary layer blockage effects (I step). The resulting flow field is then used to estimate the diffusion factor and flow blockage, from which a corrected inducer geometry is obtained and the corresponding flow field is computed. A 3D computer rendering is automatically displayed and the overall geometrical coherence of the design is assessed. If the resulting hub geometry is not considered acceptable, iteration on the operational and geometrical input data is carried out until a satisfactory geometry is obtained. At the same time, three additional checks are carried out, in order to verify that the computed values of the following parameters fall within their acceptable ranges:

- for diffusion factor: $0 < D < 0.5$ (Peterson et al.[22])
- for solidity: $\sigma < 2$ (Jakobsen[1])
- for the ratio between the incidence and the blade angles: $\alpha/\beta_b < 0.5$ (Jakobsen[1])

Once the inducer geometry has been established by means of this iterative procedure, the noncavitating pumping characteristic can be evaluated. If the resulting performance is not consistent with the requirements, the operational and geometrical input data are modified, and the whole procedure is repeated until the original specifications are met. Typically, the generation of the inducer geometry and the prediction of its flow field and head rise for a number of flow coefficients sufficient for adequately

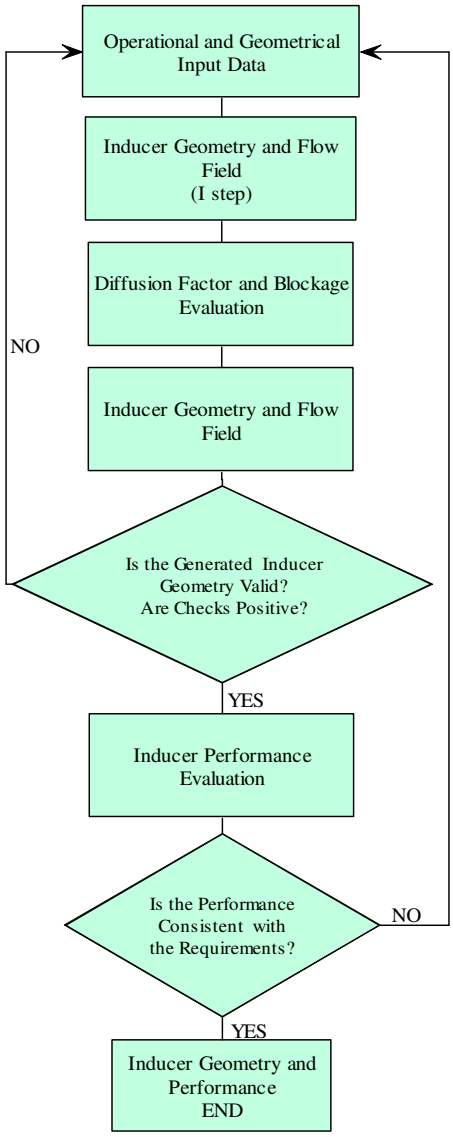

Figure 3. Flow chart of the inducer design procedure.

mapping the pumping characteristics of the inducer requires about 30 seconds on a standard desktop computer.

The application of the above procedure to the preliminary design of a specific three-bladed inducer (named DAPAMITO inducer) will now be illustrated as an example. Table 1 reports the geometrical and operational parameters of this inducer. The overall dimensions of the DAPAMITO inducer have been chosen for allowing its installation and testing in the current configuration of Alta's Cavitating Pump Rotordynamic Test Facility. As a target point of the design procedure, the performance of the MK1 Vulcain inducer has been used. This inducer, produced in Italy by Avio S.p.A. and previously tested in Alta's laboratories (Cervone et al.[23]), is a prototype of the liquid oxygen inducer of the first stage rocket engine of the Ariane 5 launcher. A moderate value of the blade loading (D = 0.39) and a high solidity (σ_T = 2.03) have been chosen for reducing the leading-edge cavity and improving the suction performance. The value of α/β_b < 0.5 has been selected with the aim of controlling the danger of surge instabilities at design flow under cavitating conditions.

Figure 4 shows a computer rendering of the DAPAMITO inducer, where the profile of the tapered hub and the variable blade pitch can be observed.

Table 1. Geometrical and operational parameters of the DAPAMITO inducer.

Design flow coefficient	[--]	Φ_D	0.059
Number of blades	[--]	N	3
Tip radius	mm	r_T	81.0
Inlet tip blade angle	deg	γ_{Tle}	83.10
Inlet hub radius (fully-developed blade)	mm	r_{Hle}	44.5
Outlet hub radius	mm	r_{Hte}	58.5
Axial length (fully-developed blade)	mm	c_a	63.5
Rotational speed	rpm	Ω	3000
Inlet hub radius	mm	r_{H1}	35.0
Axial length	mm	L	90.0
Diffusion factor	[--]	D	0.39
Ratio between the incidence and blade angles	[--]	α/β_b	0.3
Tip solidity	[--]	σ_T	2.03
Hub solidity	[--]	σ_H	2.07
Incidence tip angle @ design	deg	α	2.07
Outlet tip blade angle	deg	γ_{Tte}	74.58

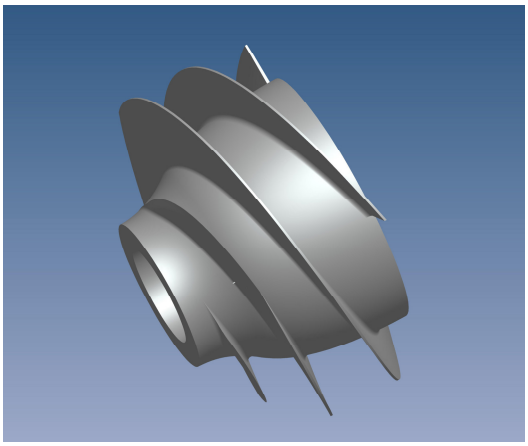

Figure 4. Computer rendering of the DAPAMITO inducer.

B. Inducer Non-Cavitating Pumping Performance

A first validation of the analytical model has been carried out by comparing its results to the experimental performance of several tapered-hub inducers tested at Alta and in Japan (d'Agostino et al.[18]). For all the cases taken into consideration, the static head rise predicted by the model closely agrees with the experimental results.

In the case of the DAPAMITO inducer, the head coefficients based on the static and total pressure rise with and without losses are reported in Figure 5 (left). The performance curves have been computed using the discharge flow field obtained by means of the closed form approximation, but it can be shown that they are essentially equivalent to those obtained by the numerical solution of the BVP (d'Agostino et al.[18]). The pressure rise is rather high if compared to that of typical space inducers, indicating that the DAPAMITO inducer can be considered an "high-head" inducer.

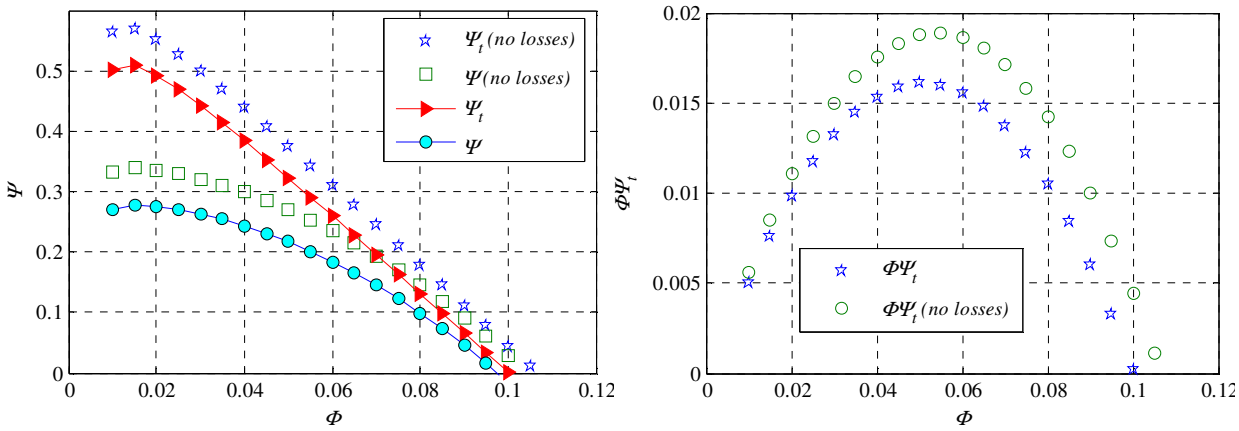

Figure 5. The noncavitating performance (left) and nondimensional hydraulic power (rigth) of the DAPAMITO inducer.

The right hand side of Figure 5 shows the non-dimensional hydraulic power generated by the DAPAMITO inducer, based on the total head coefficient evaluated with and without losses. Consistently with common engineering practice, the design flow coefficient falls just after the maximum of the power curves.

C. Inducer Discharge Flow

Figure 6 shows the axial and azimuthal flow velocity profiles as functions of the radial coordinate evaluated at the trailing edge section (*te*) of the inducer blades for three different flow coefficients (80%, 100% and 120% of the design value). The axial velocity is radially uniform, consistently with the original assumptions of the model. The azimuthal velocity includes the averaged slip vorticity correction of Figure2.

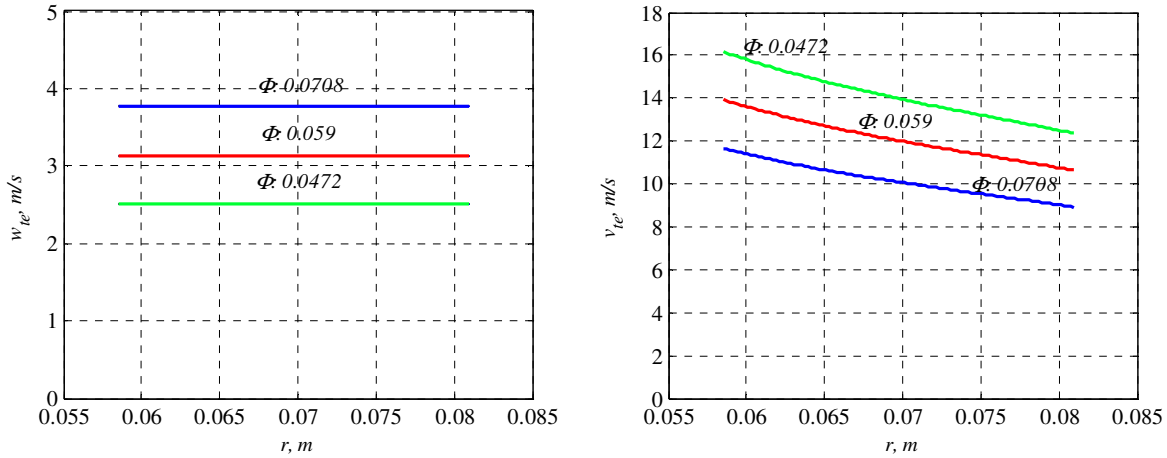

Figure 6. Axial (left) and azimuthal (right) velocity profiles at the trailing edge section (*te*) of the DAPAMITO inducer as functions of the radial coordinate evaluated for Φ_D (design flow coefficient), 0.8 Φ_D and 1.2 Φ_D.

Figure 7 shows the corresponding discharge flow angles:

$$\beta_{te} = \tan^{-1}\left(\frac{v_{te}}{w_{te}}\right)$$

as functions of the radial coordinate *r*.

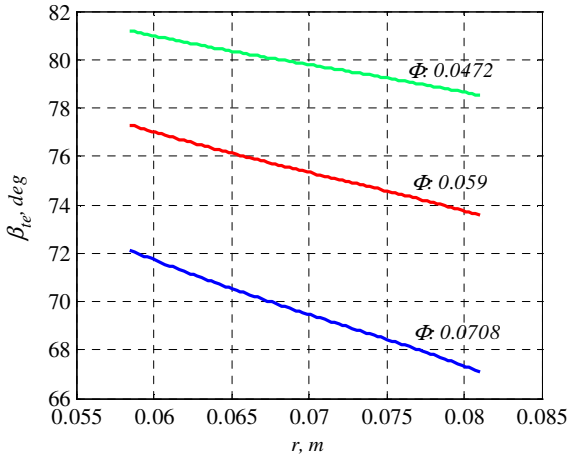

Figure 7. Discharge flow angles at trailing edge section (*te*) of the DAPAMITO inducer as functions of the radial coordinate for Φ_D (design flow coefficient), 0.8 Φ_D and 1.2 Φ_D.

III. Comparison with Numerical Simulations

A. Numerical Approach

In order to validate the results of the model, numerical simulations have been carried on the DAPAMITO inducer geometry by means of the commercial CFD software FLUENT® by Fluent Inc. The three-dimensional double precision segregated solver has been chosen to solve the Reynolds-averaged Navier-Stokes equations. For the discretization of both the turbulence and momentum equations a first order upwind scheme has been used, whereas a linear scheme has been employed for the pressure equation. So far second-order accurate solutions have experienced some convergence problems because of a zone with highly skewed cells in the mesh. A new grid generation method is currently under development in order to increase the smoothness of the geometry. The RNG k-ε turbulence model has been used for improving accuracy in the evaluation of swirling flows, and the near-wall region has been treated by means of standard wall functions. A uniform flow with a fixed axial velocity has been assigned at the duct inlet section, while a radially equilibrated pressure field with an given value on the lower boundary has been imposed at the outlet section. The incoming flow has been supposed to be turbulent with a turbulence intensity of 6%.

B. Grid Generation

Calculations have been performed on a structured hexahedral/pyramidal mesh created by means of a dedicated grid generator written in C++ programming language. The central idea has been to split the computational domain in several sub-volumes homomorphic to a prism with either a quadrilateral or triangular base. Each one of these volumes is mapped following a common scheme (see Figure 8) and then it is shaped using a proper coordinate transformation based on the inducer geometry equations. This approach allows for efficient control of the mesh size and rapid change of the geometrical parameters. Taking advantage of the periodicity of the inducer geometry, the mesh reproduces only the flow field around a single blade (see Figure 9.), in order to significantly reduce the computational time. A preliminary study has been carried out on the mesh sizing in order to find the best compromise between accuracy and computational time. About 250000 cells have been estimated to be necessary. The actual final mesh size is 245166 cells.

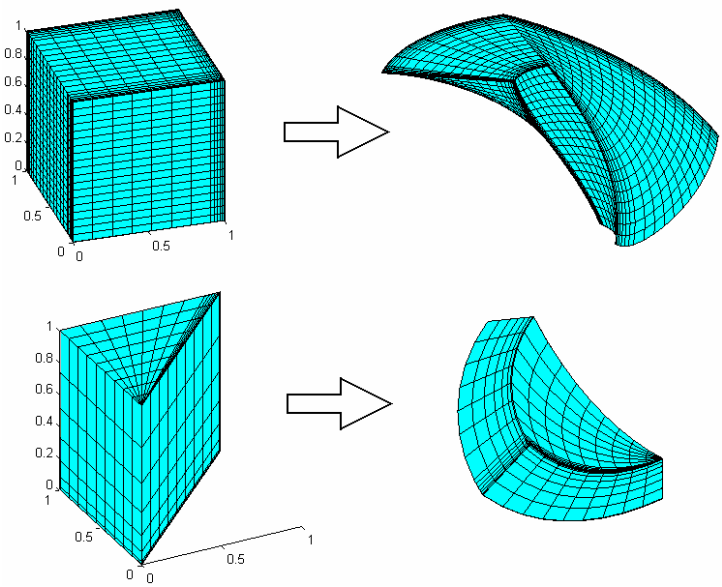

Figure 8. Example of mapping and transformation of the numerical grid sub-domains.

The computational domain has been extended 3 tip diameters upstream of the inducer leading edge in order to obtain an unperturbed flow at the inlet section. For similar reasons, the domain has been extended about one tip diameter downstream of the inducer trailing edge, where a sufficiently homogeneous flow in the azimuthal direction can be expected (see Figure 9.).

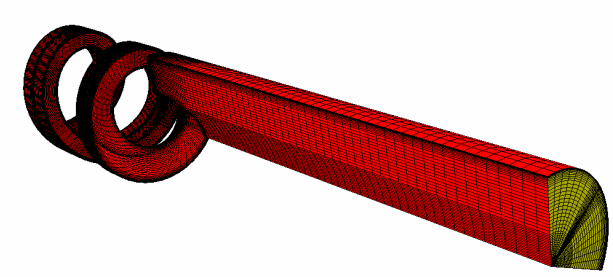

Figure 9. Mesh of the computational domain used for the DAPAMITO inducer flow simulations.

Figure 10 shows the grid generated on the surfaces of the DAPAMITO inducer. A finer mesh size has been used in correspondence of the regions where greatest gradients of the computed quantities are expected. Typically, the the prediction of its flow field and head rise for a given value of the flow coefficient requires about 12 hours on a modern desktop computer.

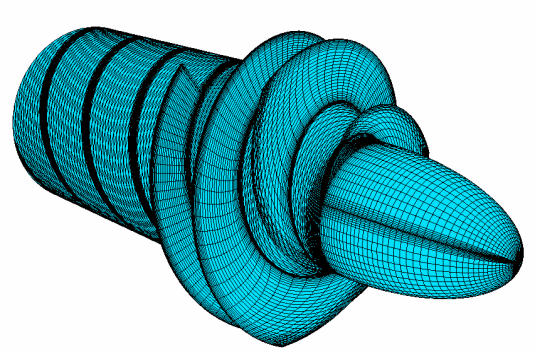

Figure 10. Computational grid generated on the surfaces of the DAPAMITO inducer.

C. Numerical Evaluation of the Inducer Flow

The exit flow field is not only necessary for correctly predicting the inducer performance, but also for proper matching with the downstream flow straightener or the centrifugal pump. As a consequence, the comparison between the model predictions and the numerical simulations has been carried out at the blade trailing edge section.

Figure 11 shows the axial velocity profile evaluated at the trailing edge section. The assumption of radial uniformity is almost satisfied, except for the obvious presence of the hub and casing boundary layers. The no-slip condition requires zero velocity on these surfaces and consequently the axial velocity profile cannot be exactly uniform in the radial direction.

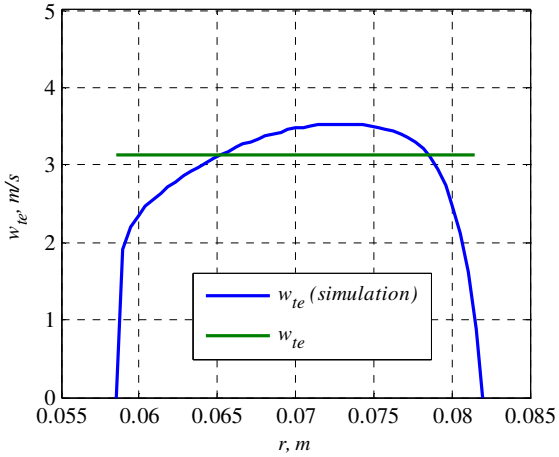

Figure 11. Comparison between the analytical and numerical axial velocity profiles at the trailing edge section (*te*) of the DAPAMITO inducer at design flow conditions.

The influence of no-slip boundary conditions on hub and casing is also evident in the mean azimuthal velocity profile (see Figure 12). This velocity is equal to zero at the casing and to the local rotational velocity at the hub. Because of the high solidity of the inducer and the presence of the boundary layers, the numerical result is not nearly linear as predicted by the model. Besides, the fully-guided azimuthal velocity obtained from the analytical model must be corrected for flow deviation effects:

$$v_{te\delta^\circ} = \Omega r_{te} - w_{te}\frac{r_{te}}{r_T}\tan\left(\gamma_{Tte} + \delta^\circ\right) + \tilde{v}_{te}$$

With this correction, the numerical and model predictions of the azimuthal velocity profiles are in substantial agreement.

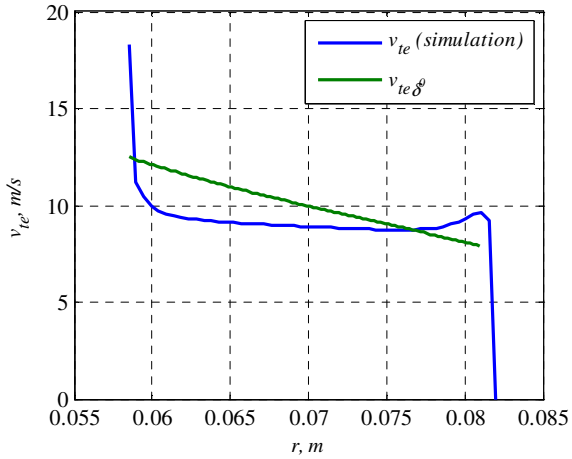

Figure 12. Comparison between the analytical and numerical azimuthal velocity profiles at the trailing edge section (*te*) of the DAPAMITO inducer at design flow conditions.

Figure 13 shows the discharge flow angles, as functions of the radius, evaluated at the trailing edge section (*te*) under design conditions. These angles are particularly important for designers, in order to assure good matching of the inducer with a downstream flow straightener. The figure shows that the reduced order model is able to closely predict the exit flow angles along the radial coordinate, at least in the locations where boundary effects are negligible.

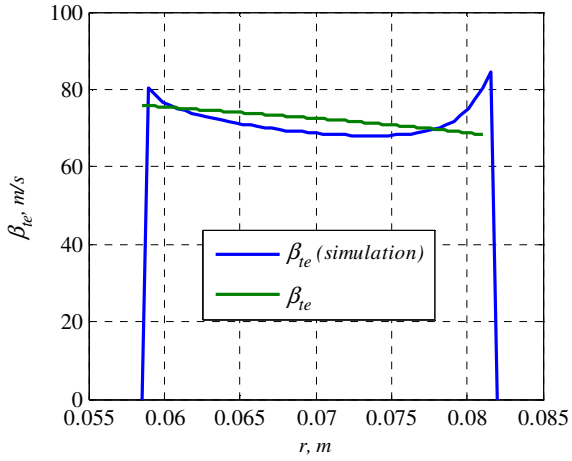

Figure 13. Comparison between the analytical and numerical discharge flow angles, as functions at the trailing edge section (*te*) of the DAPAMITO inducer at design flow conditions.

D. Numerical Evaluation of Inducer Noncavitating Pumping Performance

The numerical and analytical evaluation of the head coefficients based on the static and total pressure are reported in Figure 14 for the DAPAMITO inducer. It is worth noticing that, in the case of the head coefficient based on total pressures, the numerical solution and the corresponding closed form approximation lead to essentially equivalent results. Only for very low values of the flow coefficient ($\Phi < 0.040$) a small difference between the two curves can be observed.

Conversely, the static head coefficient is evaluated with lower accuracy. The expected noncavitating performance of the inducer, obtained by the numerical simulation, is higher than predicted by the analytical model. In this case, the discrepancy between the curves is probably due to the different evaluation of the flow velocities in the downstream section (2).

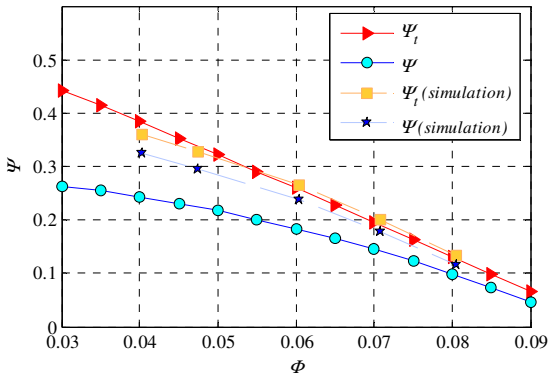

Figure 14. Comparison of the analytical and numerical noncavitating performance of the DAPAMITO inducer.

IV. Conclusions

The reduced order model presented in this paper proved to be a useful tool for the preliminary design and performance analyses of turbopump inducers. More specifically, the model is able to provide accurate quantitative indications for geometry definition, 3D flow field description, characterization and control of the blade loading, and prediction of the noncavitating pumping characteristics of helical inducers with tapered hub and variable blade pitch angle.

In a previous paper (d'Agostino et al.[18]), it has already been shown that the model is quite effective for the preliminary evaluation of the noncavitating performance of an inducer of given shape, by comparing the results of the model to the experimental results obtained on several space rocket inducers tested at Alta S.p.A. and in Japanese laboratories. The model also proved able of closely approximating the actual geometry of the high-head inducers tested at Alta S.p.A.

In the present paper, the application of the model for designing new inducers has been illustrated in detail. A high-head tapered inducer, named DAPAMITO inducer, has been designed by means of the model equations and its noncavitating performance and flow field have been evaluated and compared to those obtained by a numerical CFD computation. The results clearly show that, in spite of its inherent limitations, the model provides turbopump designers with a comprehensive interpretative framework where the main – often conflicting – design aspects of axial inducers and their mutual implications can be assessed, quantified and balanced in view of the attainment of the desired requirements and performance. Together with earlier experimental validations, the comparison with the numerical results dramatically confirms the capability of the proposed model to generate useful engineering solutions at an infinitesimal fraction of the computational cost required by 3D inducer flow simulations.

Acknowledgments

The present work has been supported by the European Space Agency under Contract No. 20081/06/NL/IA. The authors would like to express their gratitude to Profs. Mariano Andrenucci, Renzo Lazzeretti and Fabrizio Paganucci of the Dipartimento di Ingegneria Aerospaziale, Università di Pisa, Pisa, Italy, for their constant and friendly encouragement.

References

[1]Jakobsen, J. K., 1971,' "Liquid Rocket Engine Turbopump Inducers", NASA SP-8052.

[2]Ashihara, K., Goto, A., Kamijo, K., Yamada, H., Uchiumi, M., 2002, "Improvements of Inducer Inlet Backflow Characteristics Using 3-D Inverse Design Method", *38th AIAA/ASME/SAE/ASEE Joint Propulsion Conference*, Indianapolis, USA.

[3]Kang, D., Cervone, A., Yonezawa, K., Horiguchi, H., Kawata, Y., Tsujimoto, Y., 2007, "Effect of Blade Geometry on Tip Leakage Vortex of Inducer", *The 9th Asian International Conference on Fluid Machinery*, Jeju, South Korea.

[4]Brennen, C.E., 1994, "*Hydrodynamics of Pumps*", Concepts ETI, Inc. and Oxford University Press.

[5]Brennen, C.E., 1995, "*Cavitation and Bubble Dynamics*", Oxford University Press.

[6]Stripling, L.B. and Acosta, A.J., 1962, "Cavitation in Turbopumps – Part 1", *ASME J. Basic Eng*., Vol. 84, pp. 326-338.

[7]Brennen, C.E., Acosta, A.J., 1973, 'Theoretical, Quasi-Static Analysis of Cavitation Compliance in Turbopumps", *J. of Spacecraft*, Vol. 10, No. 3, pp. 175-179.

[8]Brennen, C.E., 1978, "Bubbly Flow Model for the Dynamic Characteristics of Cavitating Pumps", *J. of Fluid Mechanics*, Vol. 89, part 2, pp. 223-240.

[9]Tsujimoto, Y., Kamijo, K., Yoshida, Y., 1993, "A Theoretical Analysis of Rotating Cavitation in Inducers", *ASME J. of Fluids Engineering*, Vol. 115, pages 135-141.

[10]Tsujimoto, Y., Watanabe, S., Horiguchi, H., 1998, "Linear Analyses of Cavitation Instabilities of Hydrofoils and Cascades", *Proceedings of US-Japan Seminar: Abnormal Flow Phenomena in Turbomachinery*, Osaka, Japan.

[11]Watanabe, S., Yokota, K., Tsujimoto, Y., Kamijo, K., 1999, "Three-Dimensional Linear Analysis of Rotating Cavitation in Inducers Using an Annular Cascade Model", *ASME J. of Fluids Engineering*, Vol. 121, pp. 866-871.

[12]d'Agostino, L. and Venturini-Autieri, M.R., 2002, "Three-Dimensional Analysis of Rotordynamic Fluid Forces on Whirling and Cavitating Finite-Length Inducers", *9th Int. Symp. on Transport Phenomena and Dynamics of Rotating Machinery (ISROMAC-9)*, Honolulu, USA.

[13]d'Agostino, L. and Venturini-Autieri M.R., 2003, "Rotordynamic Fluid Forces on Whirling and Cavitating Radial Impellers", *CAV 2003*, *5th International Symposium on Cavitation*, Osaka, Japan.

[14]Semenov, Y. A., Fujii, A., Tsujimoto, Y., 2004, "Rotating Choke in Cavitating Turbopump Inducer", *ASME J. of Fluids Engineering*, Vol. 126, pp. 87-93.

[15]Cooper, P., 1967, "Analysis of Single- and Two-Phase Flows in Turbopump Inducers", *ASME J. of Engineering for Power*, October 1967, pp. 577-588.

[16]Lakshminarayana, B., 1982, "Fluid Dynamics of Inducers - A Review"*, ASME J. of Fluids Engineering*, Vol. 104, pp. 411-427.

[17]Bramanti, C., Cervone, A., d'Agostino, L., 2007, "A Simplified Analytical Model for Evaluating the Noncavitating Performance of Axial Inducers", *43rd AIAA/ASME/SAE/ASEE Joint Propulsion Conference*, Cincinnati, USA.

[18]d'Agostino, L., Torre, L., Pasini, A. and Cervone, A., "A reduced order model for preliminary design and performance prediction of tapered inducers", *12th International Symposium on Transport Phenomena and Dynamics of Rotating Machinery*, Honolulu, Hawaii, February 17-22, 2008.

[19]Hildebrand, F.B., 1976, "Advanced Calculus for Applications", 2nd edition, Prentice Hall.

[20]Lieblein, S., Schwenk, F.C. and Broderick, R.L., 1953, "Diffusion Factor for Estimating Losses and Limiting Blade Loadings in Axial Flow Compressor Blade Elements", NACA RM E53D01.

[21]Lieblein, S., 1965, "Experimental flow in Two-Dimensional Cascades", Aerodynamic Design of Axial Flow Compressors, NASA SP-36, 101-149.

[22]Peterson, C. R., Hill, P.G., 1992, "Mechanics and Thermodynamics of Propulsion", Addison –Wesley Publishing Company.

[23]Cervone, A., Testa, R., Bramanti, C., Rapposeli, E. and d'Agostino, L., 2005, "Thermal Effects on Cavitation Instabilities in Helical Inducers", *AIAA Journal of Propulsion and Power*, Vol. 21, No. 5, Sep-Oct 2005, pp. 893-899.